processes

MDPI

Article

Simulation and Parametric Evaluation of Pb (II) Adsorption in a Biomass-Packed Bed Using Isothermal Freundlich–LDF and Langmuir II–LDF Models

Angel Villabona-Ortíz [1,*], Oscar E. Coronado-Hernández [2,*] and Candelaria Tejada-Tovar [1]

[1] Process Design and Biomass Utilisation Research Group (IDAB), Chemical Engineering Department, Universidad de Cartagena, Avenida del Consulado St. 30, Cartagena de Indias 130015, Colombia; ctejadat@unicartagena.edu.co
[2] Instituto de Hidráulica y Saneamiento Ambiental, Universidad de Cartagena, Cartagena de Indias 130001, Colombia
* Correspondence: avillabonao@unicartagena.edu.co (A.V.-O.); ocoronadoh@unicartagena.edu.co (O.E.C.-H.)

Abstract: The objective of this study was to model an adsorption column bed with biomass residues using computational software to remove Pb (II) at the industrial level and analyse the effects of parametric variation. For this purpose, several simulations of the adsorption column were performed using Aspen Adsorption software, evaluating the effects of varied height, inlet flow rate, and initial concentration on the adsorption process performance. The Langmuir II and Freundlich models are established as isotherm models, and the linear driving force (LDF) model is established as the kinetic model. The findings showed that Freundlich–LDF obtained efficiencies of up to 99.9% and Langmuir II–LDF efficiencies of up to 99.7%. The optimal simulation conditions were a column height of 4 m, an initial Pb (II) concentration of 3000 mg/L, and an inlet flow rate of 250 m^3/d. This study presents a novel engineering approach to predict the potential performance of columns packed with organic waste-derived biomasses in multi-scale Pb (II) removal using computer-aided engineering tools.

Keywords: adsorption isotherm; kinetic models; Aspen Adsorption; linear global resistance model; electrolyte non-random two-liquid model

check for updates

Academic Editor: Marco Vaccari

Received: 4 April 2025
Revised: 22 May 2025
Accepted: 22 May 2025
Published: 24 May 2025

Citation: Villabona-Ortíz, A.; Coronado-Hernández, O.E.; Tejada-Tovar, C. Simulation and Parametric Evaluation of Pb (II) Adsorption in a Biomass-Packed Bed Using Isothermal Freundlich–LDF and Langmuir II–LDF Models. *Processes* **2025**, *13*, 1655. https://doi.org/10.3390/pr13061655

Copyright: © 2025 by the authors. Licensee MDPI, Basel, Switzerland. This article is an open access article distributed under the terms and conditions of the Creative Commons Attribution (CC BY) license (https://creativecommons.org/licenses/by/4.0/).

1. Introduction

The increasing pollution of water bodies is due to various factors but primarily generated by industries such as mining, textiles, paper manufacturing, fertilisers, paints, and oil refining. These industries are considered key drivers of rapid industrialisation, which boosts the economy and improves human well-being [1]. However, industrial activities have significantly increased the production of wastewater containing various contaminants, raising concerns about the pollution of water resources.

Among these contaminants are heavy metals, which, upon contact, exist in various chemical states or forms and accumulate in different environmental zones, such as water bodies, sediments, and soils, after being released into the environment. This occurs because heavy metals possess a characteristic that makes them incapable of biodegradation. Consequently, heavy metal ions generated by industrial waste have accumulated over time, leading to their absorption by living organisms and causing adverse effects on human health, animals, and the environment [2,3].

Lead (Pb) is a prevalent heavy metal that occurs naturally in the Earth's crust as well as in food, paints, and other materials. This heavy metal is strongly neurotoxic to the human

body and can cause respiratory, digestive, and neurological problems. Additionally, due to its high toxicity, it can induce cellular mutations, leading to the formation of cancerous cells and various metabolic and physiological disorders in humans, animals, and plants [4,5]. Pb (II) is one of the most widely used elements in various industries, including electroplating, painting, steel production, batteries, smelting, inorganic fertilisers, pesticides, and the food industry. The latter is a major contributor to lead consumption due to its canned products and the leaching characteristics of canned foods [6]. In Colombia, Law 41 of 2020 stipulates that the maximum allowable lead concentration in water is 0.0005 mg/L [7].

One of the most important research topics investigated is wastewater treatment. Different techniques and processes have been developed which can be physical, chemical, and/or biological to remove, eliminate, or neutralise a wide range of pollutants present in effluent, such as suspended solids, colloid particles, organic matter, nutrients, and dissolved contaminants such as heavy metals and organic compounds. Among the different techniques for the treatment of wastewater loaded with heavy metals such as Pb (II) are the following: The coagulation/flocculation process that implements coagulants or flocculants, whether chemical or natural, that seek to destabilise and group suspended particles—colloids, heavy metals, colorants, among others—present in the water, facilitating their elimination [8]. Electrocoagulation is an advanced water treatment technique that involves the destabilisation and subsequent aggregation of suspended, emulsified, or dissolved contaminants through the application of a low-voltage direct current across sacrificial electrodes, commonly composed of aluminum or iron [9].

Among all these techniques, adsorption is presented as an effective method to remove the desired contaminants, standing out for its ease of scalability and feasibility. This is a process in which a solute (adsorbate) binds to the surface of a solid material (adsorbent) due to the action of attractive forces until it reaches an equilibrium state in which the amount of adsorbate retained stops increasing. It can also be described as forming an adsorbate layer on the adsorbent, driven by interactions such as Van der Waals forces. This phenomenon involves the preferential accumulation of adsorbate at the solid–liquid interface compared to its concentration in the liquid phase. The adsorbent used in this process is a porous material with a large surface area, favouring a higher retention capacity. This removal technique has been widely employed in numerous studies to eliminate and recover heavy metals from wastewater, even at low concentrations, due to its practicality and ease of implementation compared to other water treatment methods [10,11].

The adsorption mechanism begins when the contaminated solution transports the adsorbate molecules to the boundary layer of the adsorbent. Then, diffusion occurs from the boundary layer to the outer surface of the adsorbent. Finally, the contaminant molecules are transported from the outer surface to the active sites within the adsorbent's pores, where the contaminant ions are fixed [12]. Adsorption is classified into physical (physisorption) and chemical (chemisorption) types. In physisorption, the process is driven by short-range electrostatic forces, such as Van der Waals interactions, which generate a weak attraction between the adsorbate and the adsorbent. In chemisorption, on the other hand, adsorption involves the formation of chemical bonds between the two species, resulting in a stronger and more specific interaction. This chemical bonding is more challenging to reverse and requires more energy to desorb the molecules than physical adsorption [13].

To understand the interactions that arise between adsorbate and adsorbent during the adsorption process, mathematical models (Isothermal models) have been developed, which play a crucial role in optimising the use of any adsorbent [14]. Among the different models are Langmuir's isothermal model, which describes how a solute binds to a solid surface, generating a monolayer with homogeneous active sites [15], and Freundlich's isothermal model, which establishes adsorption as a process that occurs on a multilayer

surface with homogeneous active sites [16]. Most adsorption studies have been conducted at the laboratory scale. Consequently, efforts have been made to predict adsorption process behaviour on a larger scale and understand how these changes affect the efficiency of the adsorbent material. Studies have been carried out using computational tools to model industrial-scale adsorption columns. However, research on this topic remains limited, indicating that it is still in its early stages.

Therefore, this study seeks to remove Pb (II), which poses a serious risk to human health and the environment, and exposure to which can cause severe damage to the nervous system, kidneys, and blood and is especially harmful to children and pregnant women. To achieve this, Cacao (*Theobroma cacao* L.) was selected as a packing material for the Pb (II) removal column for its wide production in Colombia and the significant residual biomass it generates. This biomass mainly comprises the husk of the cob, the husk of the bean, and the pulp. Among these by-products, cocoa husk stands out for its availability, low cost, and renewable nature, making it suitable for adsorption columns. Its high cellulose (19.82%), hemicellulose (9.45%), and lignin (12.66%) content gives it a high adsorbent capacity, which makes it a sustainable and effective alternative for the removal of pollutants in aqueous media.

To find ways to mitigate the impact caused by this pollutant, this study aims to model an industrial-scale packed adsorption column for Pb (II) using computational software and analyse the effects of parametric variation based on experimental data previously obtained by the authors using *Theobroma cacao* L. as adsorbent material. It will present the simulation of Pb (II) adsorption processes in a column using Aspen Adsorption, which models the behavior of multiscale adsorption columns, facilitating the prediction of performance at the laboratory, pilot, and industrial scales in the removal of contaminants, simulating key phenomena such as mass transfer, adsorption equilibrium and fluid dynamics and optimising the design and operation of the system based on experimental parameters. Its application in treating lead-contaminated water allows for evaluating different operating conditions, improving process efficiency, and transitioning effectively from multi-scale studies, i.e., from laboratory- to industrial-scale implementation.

2. Materials and Methods

2.1. Biomaterial Preparation and Experimental Adsorption Tests

The cocoa residues were rigorously washed to eliminate dirt. They were then dried at 95 °C for 24 h using in an Isotherm® OFA-32-8 forced convection laboratory oven manufactured by ESCO, Singapore–Southeast Asia, to eliminate excess moisture. Subsequently, the dry material was ground using a conventional stainless steel hand mill and then sieved on an AISI 316 stainless steel laboratory sieve manufactured by FILTRA VIBRACION, S.L, Barcelona, Spain, with a particle size of 0.5 mm. All of this equipment was located in the Physical Chemistry Laboratory of the Universidad de Cartagena, Piedra de Bolivar, Cartagena, Colombia.

The experimental setup was based on a typical configuration for studying heavy metal adsorption in a continuous flow system. Unlike batch adsorption experiments, in which the solution and adsorbent are mixed in a closed vessel, continuous adsorption studies simulate more realistic conditions in which the contaminated solution constantly flows through a packed bed column filled with cocoa waste. The experiment was conducted using a fixed packed bed of 6.6 cm diameter operating at 25 °C with pH 6 and an initial concentration of Pb (II) of 100 ppm prepared using lead salts (Lead Nitrate ($Pb(NO_3)_2$)—analytical grade 99%, manufactured by Loba chemie–Bombay, India) to generate synthetic contaminated water. In addition, a plug-type peristaltic flow pump was used to maintain a constant flow rate with a value of 1 mL/s.

On the other hand, packed column depth ranges of 4 and 7.5 cm were used to evaluate their effects on the performance of the adsorption process. Samples were taken from the bottom of the packed bed at 10, 30, 60, 90, 120, 150, 180, 210, 240, and 270 min. Finally, contaminant concentrations were determined by UV–Vis spectroscopy to evaluate the performance of the adsorption bed through breakthrough curves analysis using a breakthrough point defined at 5% of the initial concentration (C/Co = 0.05) corresponding to the process efficiency of 95% [17].

Subsequently, the reusability and regeneration capacity of the adsorbent for the pollutant were evaluated by performing a cyclic adsorption–desorption process using NaOH and HCl solutions. The desorption process started by taking a mass quantity of 0.5 g of the biomass recovered from the adsorption processes and placing it in contact with acid and base solutions of 0.2 M HCl and 0.2 M NaOH in a mechanical stirrer for 2 h at 140 rpm. The adsorbent material was washed with distilled water and left to dry in an oven at 100 °C for 20 min. Then, the adsorption process was repeated in a Pb (II) solution at 100 mg/L and mounted in rotating equipment for 2 h at 140 rpm. Finally, the material was filtered, and the absorbance was measured in a UV–vis spectrophotometer [18].

2.2. Simulation and Adsorption Column Configuration

To simulate the packed column for Pb (II) adsorption, the necessary thermodynamic package must first be established to calculate the physical properties of the substance entering the column. For this study, the ELECNRTL (electrolyte non-random two-liquid) method was employed to determine the physical properties of the feed stream in the adsorption column. This method allows the handling of aqueous electrolyte solutions at both low and high concentrations provided that no vapour phase is present in the mixture [19].

Next, the adsorption column was configured in Aspen Adsorption, which consists of various sections essential for correctly defining the simulation conditions:

- General: This section requires selecting the discretisation method to run the adsorption process simulation. This study employed the Upwind Differencing Scheme 1 (UDS1) method, which utilised 10 nodes.
- Mass/Momentum Balance: Here, the basic assumptions regarding axial dispersion in the liquid phase are defined, as well as how pressure drop is handled in the adsorption column model and whether velocity remains constant or varies along the column. For this study, it was assumed that there is no pressure drop, convection occurs solely in the liquid phase, and velocity remains constant.
- Kinetic Model: This section determines the kinetic model used to describe the rate of the adsorption process. In this case, the linear driving force (LDF) model was selected. This model assumes that mass transfer is driven by a function of concentration and describes the rate at which the contaminant is adsorbed [20].
- Isotherm Model: This section establishes the model used to describe interactions between the adsorbate and the adsorbent. For this study, the Freundlich and Langmuir II isotherm models were selected [21–23].
- Energy Balance: This section defines how the energy balance is performed. For this case, an isothermal energy balance was applied.

2.3. Parametric Evaluation in the Adsorption Column

Using Aspen Adsorption as a simulation tool for the adsorption column to remove Pb (II) from wastewater, a parametric evaluation was conducted to assess the impact of varying the following parameters:

- Initial concentration (2000 mg/L and 3000 mg/L) [24,25];

- Adsorption column height (3 m and 4 m) [26];
- Inlet flow rate (150 m^3/d and 250 m^3/d) [26].

Figure 1 summarises the methodology presented above for implementing the Aspen Adsorption V11 software and developing the packed column for Pb (II) adsorption.

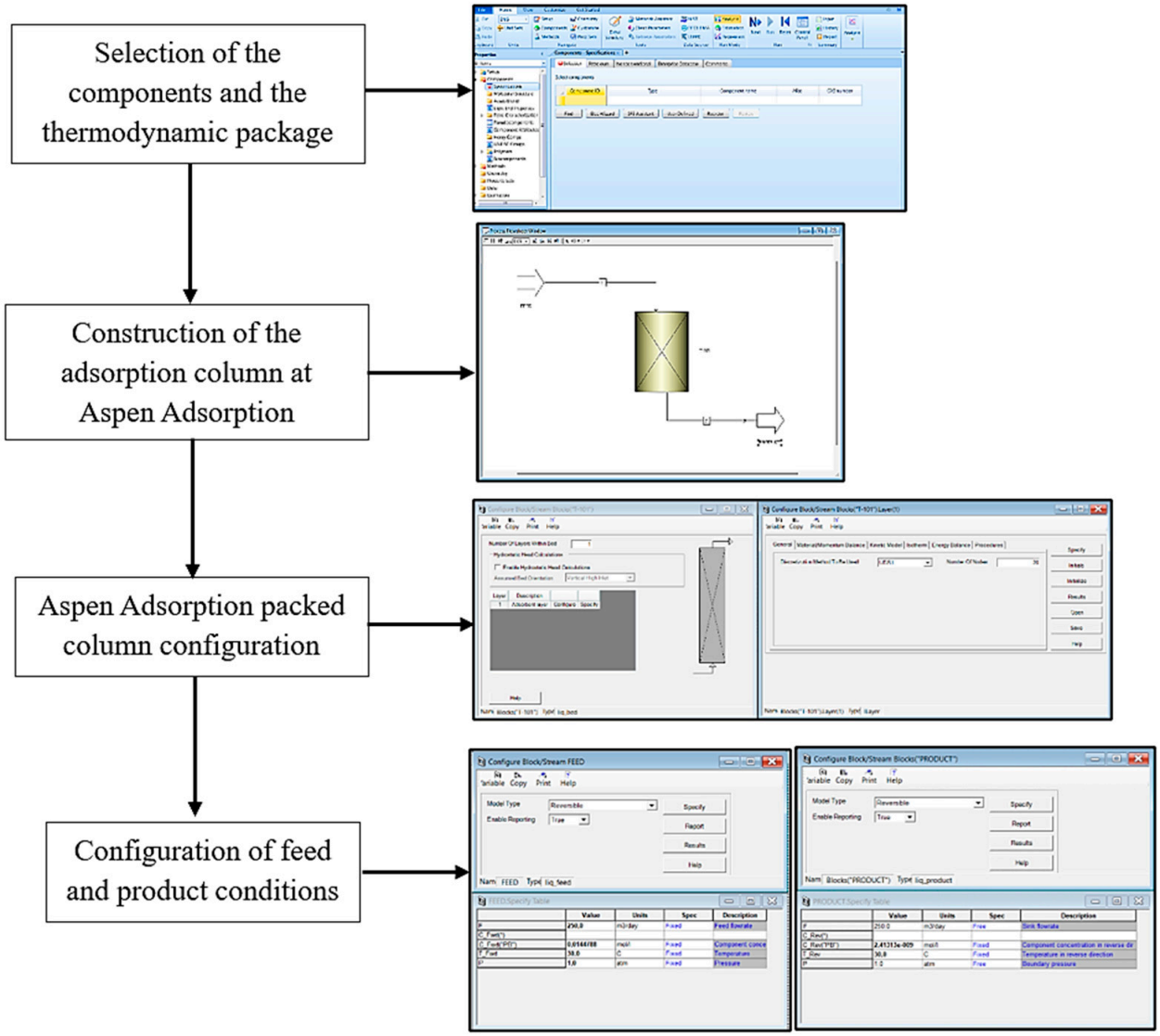


Figure 1. Methodology implemented for the simulation of the adsorption column in Aspen Adsorption.

2.4. Mathematical Fundamentals

Aspen Adsorption uses different equations embedded in its database to perform the calculations necessary for adsorption process simulation. This software performs the mass balance of the adsorption column using a partial difference equation, as shown in Equation (1), to express the metal ion concentration in a small control volume within the adsorbent column [27].

$$\varepsilon_i E_i \frac{\delta^2 C_i}{\delta z^2} + \frac{\delta}{\delta z}(v_i c_i) + \varepsilon_i \frac{\delta C_i}{\delta t} + \rho_s \frac{\delta q}{\delta t} = 0 \quad (1)$$

On the other hand, adsorption isotherms are those that describe how the adsorption process takes place when an adsorbate and an adsorbent are put in contact. For this study,

the Freundlich (Equation (2)) [16] and Langmuir II (Equations (3) and (4)) [21,23] models were selected.

$$q_e = k_f C_e^{1/n} \tag{2}$$

$$q_e = \frac{q_{m,i} b_i P_i}{1 + b_i P_i} \tag{3}$$

$$b_i = b_{0,i} \exp\left(-\Delta H / (R_g T_S)\right) \tag{4}$$

To describe the speed at which contaminant removal occurs, the software uses models describing the adsorption kinetics to predict the removal rate, evaluate the efficiency of the adsorbent used, and understand the mass transfer process. Among the models handled by Aspen Adsorption, one model was selected for this study, the LDF model, which expresses that the mass transfer driving agent possessed by the components is represented by a linear function of the concentration of the component in solid or liquid state [28]. This model is described by Equation (5):

$$\frac{\partial w_k}{\partial_t} = MTC_{sk}\left(w_k^* - w_k\right) \tag{5}$$

3. Results and Discussion

3.1. Establishment of Baseline Conditions for Column Simulation

A baseline simulation was established to configure the adsorption column for Pb (II) removal using *Theobroma cacao* L. waste. Table 1 presents the specification values required for the adsorption column in Aspen Adsorption. These values remained fixed for all configurations used in the adsorption process simulation.

Table 1. Specification values required for the adsorption column.

Parameter	Value	Reference
Adsorption column diameter (m)	1	[19]
Adsorption column porosity (m^3 of void/m^3 of column)	0.67	[29]
Bulk density (g/cm^3)	0.0365	[30]
Mass transfer coefficient (1/s)	1.88×10^{-7}	[31]
Total void porosity	0.4	[29]
Freundlich Isotherm Model Parameters		
K_F (mg g^{-1} (mg $L^{-1})^{1}/^{n}$)	0.453	[32]
$1/n$	1.476	[32]
Langmuir II Isotherm Model Parameters		
$q_{m,i}$ (mg/g)	46930.9	[21,23]
$b_{0,i}$ (bar^{-1})	8.18×10^{-7}	[21,23]
$-\Delta H/R_g$ (J/mol) (J/mol*K)$^{-1}$	1072.83	[21,23]
b_i (bar^{-1})	0.0000318	[21,23]
T_s (K)	303.15	[21,23]
P_i (bar)	1	[21,23]

Figure 2 illustrates the packed column flow diagram for the adsorption process and the concentration ratio profile at the outlet when using residues of *Theobroma cacao* L. as the adsorbent material.

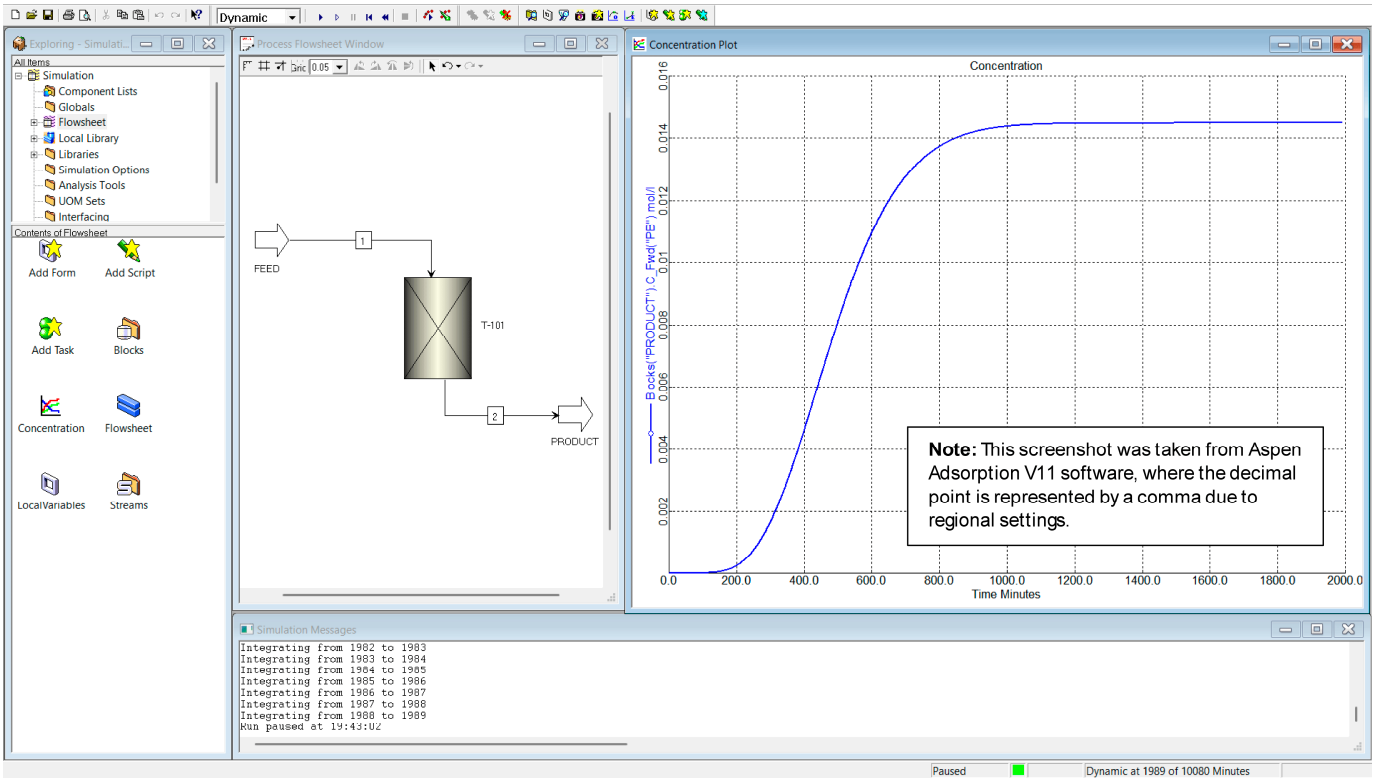


Figure 2. Flow diagram of the adsorption process and Pb (II) concentration curve profile for the adsorbent material.

3.2. Data Obtained from the Adsorption Process Simulation

Using the baseline simulation conditions configured in Aspen Adsorption, multiple large-scale packed column simulations were executed for Pb (II) removal, testing various parametric configurations of column height, initial concentration, and inlet flow rate. The adsorption process was modelled using the Langmuir II and Freundlich isotherm models and the linear driving force (LDF) kinetic model. The breakthrough and saturation times obtained for the Freundlich–LDF model are presented in Table 2.

Table 2. Simulation results for the Freundlich–LDF model.

Flow Rate (m^3/d)	Column Height (m)	Concentration (mg/L)	Breakthrough Time (min)	Saturation Time (min)
150	3	2000	492	2253
	4	2000	658	2936
	3	3000	935	1971
	4	3000	1244	2560
250	3	2000	294	1371
	4	2000	393	1823
	3	3000	563	1223
	4	3000	749	1609

On the other hand, Table 3 presents the breakthrough and saturation times obtained for the Langmuir II–LDF model.

Table 3. Simulation results for the Langmuir II–LDF model.

Flow Rate (m^3/d)	Column Height (m)	Concentration (mg/L)	Breakthrough Time (min)	Saturation Time (min)
150	3	2000	492	2256
	4	2000	659	2938
	3	3000	449	1962
	4	3000	601	2548
250	3	2000	294	1370
	4	2000	393	1825
	3	3000	267	1216
	4	3000	358	1596

3.3. Effect of Initial Pb (II) Concentration Variation

The impact of changing the initial Pb (II) concentration on adsorption was analysed using concentrations of 2000 mg/L and 3000 mg/L, with a flow rate of 250 m^3/d and an adsorption column height of 3 m. Figure 3 presents the breakthrough curves for the Freundlich and Langmuir II isotherms combined with the LDF kinetic model.

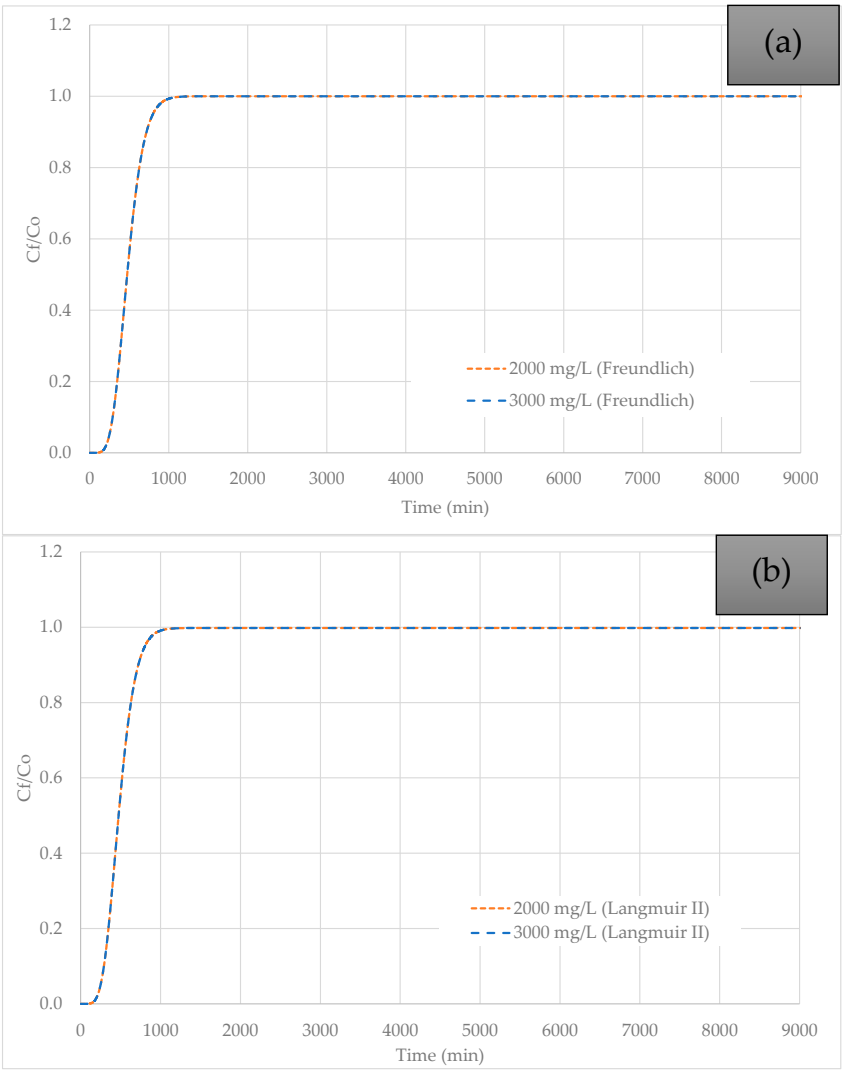


Figure 3. Breakthrough profiles for initial Pb (II) concentration variation in: (**a**) Freundlich–LDF; and (**b**) Langmuir II–LDF.

It can be observed that increasing the initial contaminant concentration prolonged the breakthrough time but reduced the saturation time. This behaviour is evident in Tables 2 and 3 and in Figure 2, where, for the Freundlich–LDF model at 2000 mg/L, the breakthrough time was 294 min, and the saturation time was 1371 min. However, at 3000 mg/L, the breakthrough and saturation times were 563 and 1223 min, respectively.

Similarly, for the Langmuir II–LDF model, the breakthrough and saturation times were 294 and 1370 min, respectively, for an initial Pb (II) concentration of 2000 mg/L. At 3000 mg/L, these times decreased to 267 and 1216 min, respectively.

The Freundlich–LDF model's adsorption efficiencies were 99.9% at 2000 mg/L and 3000 mg/L. Meanwhile, the Langmuir II–LDF model achieved an efficiency of 99.7% for both concentrations [33,34].

This trend can be attributed to the increased contaminant load, which leads to a higher occupation of active adsorption sites on the adsorbent. As a result, equilibrium is reached more rapidly, causing earlier saturation of the adsorption column.

These findings indicate that there are no significant differences in the efficiencies obtained with the Langmuir II and Freundlich models, suggesting that both models are suitable for describing the adsorption process.

3.4. Effect of Inlet Flow Rate Variation

The effect of varying the inlet flow rate on adsorption was analysed using flow rates of 150 and 250 m^3/d, with a constant initial Pb (II) concentration of 3000 mg/L and an adsorption column height of 3 m. The results, presented in Tables 2 and 3 and Figure 4, which shows the breakthrough curve profile for the Langmuir II and Freundlich models with the LDF kinetic model, reveal that increasing the inlet flow rate reduces both breakthrough and saturation times.

This can be seen in the data: for the Freundlich–LDF model, at an inlet flow rate of 150 m^3/d, the breakthrough time was 935 min, and the saturation time was 1971 min. However, for a flow rate of 250 m^3/d, the breakthrough and saturation times decreased to 563 and 1223 min, respectively. A similar trend was observed with the Langmuir II–LDF model: for 150 m^3/d, the breakthrough time was 449 min, and the saturation time was 1962. In contrast, for 250 m^3/d, the breakthrough and saturation times were reduced to 563 and 1223 min, respectively.

This time reduction can be attributed to the increased flow velocity, which leads to faster saturation of the adsorbent pores.

The Freundlich–LDF model's adsorption efficiencies were 99.9% for 250 m^3/d and 99.5% for 150 m^3/d, while the Langmuir II–LDF model's efficiencies were 99.7% for 250 m^3/d and 98.9% for 150 m^3/d [35,36].

These results indicate no significant differences in the efficiencies obtained using the Langmuir II and Freundlich models, suggesting that both models are suitable for describing adsorption processes.

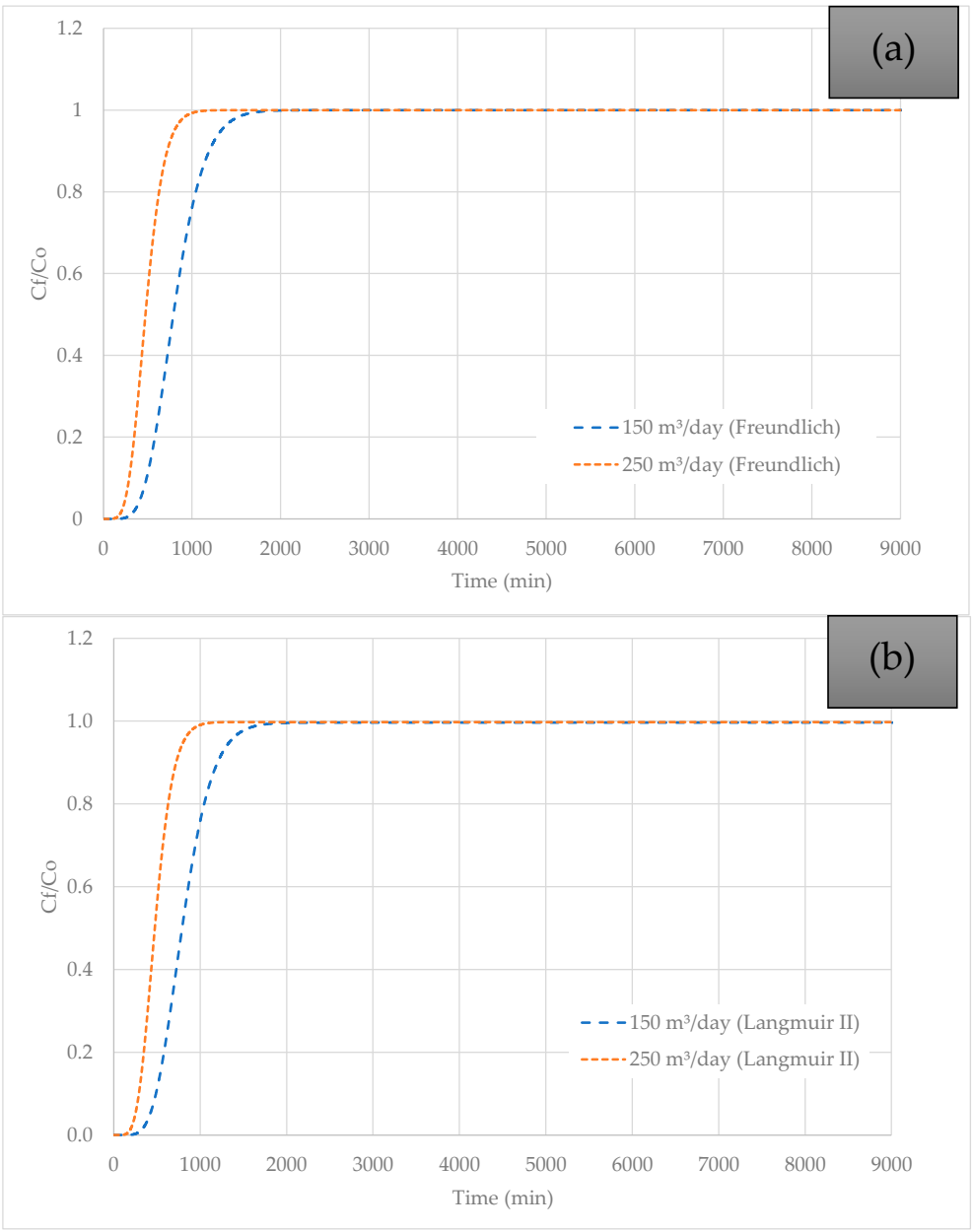


Figure 4. Breakthrough profiles for inlet flow rate variation in (**a**) Freundlich–LDF and (**b**) Langmuir II–LDF.

3.5. Effect of Column Height Variation

An analysis was conducted on the impact generated by variation in the height of the adsorption column in the adsorption process, employing column heights of 3 and 4 m with constant initial concentration and inlet flow rate, with magnitudes of 3000 mg/L and 250 m^3/d, respectively, for the Freundlich and Langmuir II models combined with the LDF model. It was demonstrated that reducing the height of the adsorption column resulted in decreased break and saturation times. This can be seen in Tables 2 and 3, and Figure 5, where, for Freundlich–LDF using a column height of 4 m, the break and saturation times were 749 and 1609 min, respectively, while with a height of 3 m, the break time was 563 min and the saturation time was 1223 min. This behaviour was repeated for the Langmuir II–LDF model, where, with a height of 4 m, the break time was 358 min and the saturation time was 1596 min, whereas for a height of 3 m, these times were 267 and 1216 min for the break and saturation times, respectively. This occurs because, with a decrease in the

height of the adsorption column, there is a smaller surface area of the adsorbent biomaterial, leading to the rapid occupation of the active sites present in the adsorbent, which results in a reduction in the breakthrough and saturation times. The adsorption process efficiencies for Freundlich–LDF were 99.9% for 3 m and 99.7% for 4 m. On the other hand, Langmuir II–LDF achieved an efficiency of 99.7% for 3 m and 99.1% for 4 m [37]. These results indicate no significant differences in the efficiencies obtained by the Langmuir II and Freundlich models, suggesting that both models are suitable for describing adsorption processes.

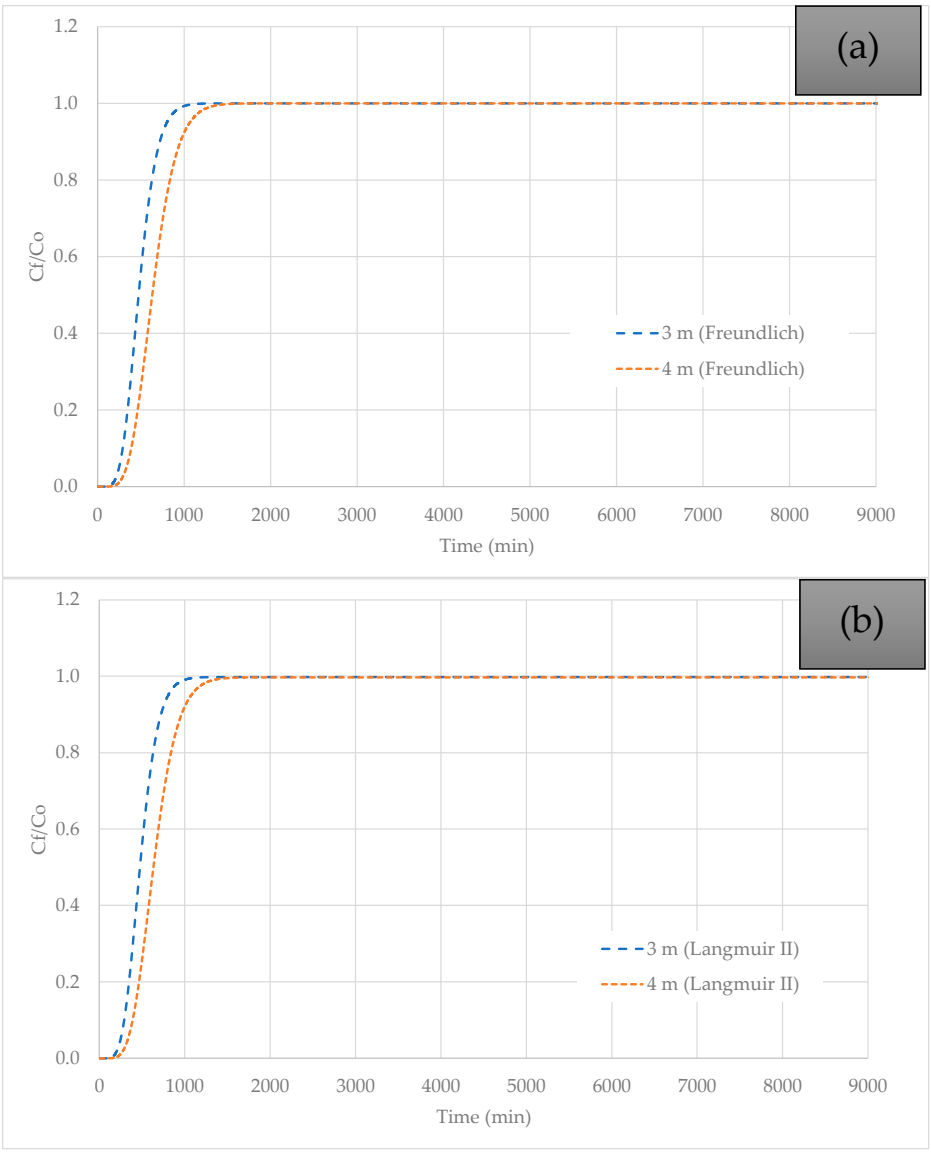


Figure 5. Breakthrough profiles of the alteration in column height for (**a**) Freundlich-LDF and (**b**) Langmuir II-LDF.

The results obtained from changes in the inlet flow rate, column height, and initial concentration confirm that the inlet flow rate was the parameter that most significantly affected the process, followed by the column height and, finally, the initial concentration of Pb (II).

3.6. Comparison with Other Results Found in the Literature

The results of the industrial-scale simulation of the packed bed with *Theobroma cacao* L. have been contrasted with studies reported in the literature. It is important to note that this

comparison has relative value, since each study was carried out under different conditions of inlet flow, initial concentration, bed height, and type of adsorbent biomaterial used. The findings of this work indicate that *Theobroma cacao* L. in an industrial-scale packed bed shows acceptable performance in removing Pb (II) in aqueous solutions. Table 4 compares the values obtained in this study with those reported in the literature.

Table 4. Comparison of the results with the literature.

Parameter	Pb (II)	Pb (II)	Pb (II)
Adsorbent	Olive tree pruning	Activated carbons	*Theobroma cacao* L.
Initial concentration (mg/L)	100	500	3000
Inlet flow rate (m^3/day)	128.04	42.68	250
Bed height (m)	2.26	0.4	3
Rupture time (min)	201.6	18	563
Saturation time (min)	503	-	1223
Source	[38]	[37]	This study

The results presented in this study contribute significantly to the scientific literature by providing relevant information on the development of the simulation of packed biomass columns for the removal of pollutants in water bodies, highlighting its novelty in the simulation of processes to reduce the existing gap in the use of agro-industrial waste at the industrial scale—in this case, the implementation of *Theobroma cacao* L. as adsorbent material—to affect the removal of Pb (II) present in wastewater. In addition, cocoa residues present significant advantages such as high abundance, low cost, good versatility, low environmental impact, and excellent adsorption capacity, making them a good raw material for producing adsorbent materials. The potential of Aspen Adsorption software as a computational tool for predicting the performance of packed adsorption columns is also demonstrated, highlighting that, in addition to metal ions, dyes and emerging contaminants can also be simulated in the software [39].

4. Conclusions

This study is presented as a valuable contribution to the scientific literature, offering a novel approach to predicting the behaviour of adsorption columns. It provides useful data for developing packed biomass column simulations to remove contaminants from water bodies. A parametric sensitivity analysis was conducted using break curve profiles derived from data obtained through multiple adsorption column simulations developed with Aspen Adsorption. The study investigated the influence of variations in initial concentration, inlet flow rate, and column height on break time, saturation time, and the efficiency of the adsorption process using the Langmuir II–LDF and Freundlich–LDF mathematical models. The results demonstrated excellent adsorption efficiency for Pb (II).

Author Contributions: Conceptualization, A.V.-O. and C.T.-T.; methodology, A.V.-O. and C.T.-T.; formal analysis, A.V.-O. and C.T.-T.; writing—original draft preparation, O.E.C.-H.; writing—review and editing, A.V.-O. and C.T.-T. All authors have read and agreed to the published version of the manuscript.

Funding: This research received no external funding.

Data Availability Statement: The original contributions presented in this study are included in the article. Further inquiries can be directed to the corresponding author.

Conflicts of Interest: The authors declare no conflicts of interest.

Abbreviations

q_e	Adsorption capacity of contaminant (mg/g)
k_f	Freundlich constant indicating adsorption capacity ((mg/g) (mL/g)^n)
C_e	Concentration of contaminant in solution at equilibrium (mg/L)
$1/n$	Effect of initial concentration on adsorption capacity.
q^*	Adsorption capacity (mg/g)
$q_{m,i}$	Maximum adsorption capacity (mg/g)
b_i and $b_{0,i}$	Langmuir II affinity constants (bar^{-1})
ΔH	Isosteric heat of adsorption of the solution (J/mol)
R_g	Gas constant (J/mol*K)
P_i	system pressure (bar)
T_S	Solution temperature (K)
ε_i	Porosity of the column
E_i	Longitudinal dispersion coefficient (m^2/s)
z	Bed length (m)
q	Amount of metal ions adsorbed by the adsorbent (mg/g)
C_i	Contaminant concentration in the liquid phase (mg/L)
ρ_s	Apparent density of the adsorbent (g/cm^3)
v_i	Speed at which the fluid passes through the bed (m/s).
w_k	Concentration adsorbed on the solid for component k (mg/g).
w_k^*	Amount that should be adsorbed if the system were in instantaneous equilibrium with the fluid phase (mg/g).
MTC_{sk}	Mass transfer coefficient (1/s).

References

1. Ismail, W.N.W.; Syah, M.I.A.I.; Muhet, N.H.A.; Bakar, N.H.A.; Yusop, H.M.; Samah, N.A. Adsorption Behavior of Heavy Metal Ions by Hybrid Inulin-TEOS for Water Treatment. *Civ. Eng. J.* **2022**, *8*, 1787–1798. [CrossRef]
2. Chen, Z.; Zhao, Y.; Liang, N.; Yao, Y.; Zhao, Y.; Liu, T. Pollution, Cumulative Ecological Risk and Source Apportionment of Heavy Metals in Water Bodies and River Sediments near the Luanchuan Molybdenum Mining Area in the Xiaoqinling Mountains, China. *Mar. Pollut. Bull.* **2024**, *205*, 116621. [CrossRef]
3. Dhobi, S.H.; Neupane, D.; Koirala, S.; Das Mulmi, D. Waste Tea as Absorbent for Removal of Heavy Metal Present in Contaminated Water. *Heliyon* **2024**, *10*, e39519. [CrossRef] [PubMed]
4. Zhao, H.; Ouyang, X.K.; Yang, L.Y. Adsorption of Lead Ions from Aqueous Solutions by Porous Cellulose Nanofiber–Sodium Alginate Hydrogel Beads. *J. Mol. Liq.* **2021**, *324*, 115122. [CrossRef]
5. Kumar, V.; Dwivedi, S.K.; Oh, S. A Critical Review on Lead Removal from Industrial Wastewater: Recent Advances and Future Outlook. *J. Water Process Eng.* **2022**, *45*, 102518. [CrossRef]
6. Raj, K.; Das, A.P. Lead Pollution: Impact on Environment and Human Health and Approach for a Sustainable Solution. *Environ. Chem. Ecotoxicol.* **2023**, *5*, 79–85. [CrossRef]
7. Amini, M.; Afyuni, M.; Khademi, H.; Abbaspour, K.C.; Schulin, R. Mapping Risk of Cadmium and Lead Contamination to Human Health in Soils of Central Iran. *Sci. Total Environ.* **2005**, *347*, 64–77. [CrossRef]
8. Badawi, A.K.; Salama, R.S.; Mostafa, M.M.M. Natural-based coagulants/flocculants as sustainable market-valued products for industrial wastewater treatment: A review of recent developments. *RSC Adv.* **2023**, *13*, 19335–19355. [CrossRef]
9. Boinpally, S.; Kolla, A.; Kainthola, J.; Kodali, R.; Vemuri, J. A state-of-the-art review of the electrocoagulation technology for wastewater treatment. *Water Cycle* **2023**, *4*, 26–36. [CrossRef]
10. Rashid, R.; Shafiq, I.; Akhter, P.; Iqbal, M.J.; Hussain, M. A State-of-the-Art Review on Wastewater Treatment Techniques: The Effectiveness of Adsorption Method. *Environ. Sci. Pollut. Res.* **2021**, *28*, 9050–9066. [CrossRef]
11. Musah, M.; Azeh, Y.; Mathew, J.; Umar, M.; Abdulhamid, Z.; Muhammad, A. Adsorption Kinetics and Isotherm Models: A Review. *Caliphate J. Sci. Technol.* **2022**, *4*, 20–26. [CrossRef]
12. Sukmana, H.; Bellahsen, N.; Pantoja, F.; Hodur, C. Adsorption and Coagulation in Wastewater Treatment—Review. *Progress. Agric. Eng. Sci.* **2021**, *17*, 49–68. [CrossRef]
13. Taiwo, A.; Chinyere, N. Sorption Characteristics for Multiple Adsorption of Heavy Metal Ions Using Activated Carbon from Nigerian Bamboo. *J. Mater. Sci. Chem. Eng.* **2016**, *4*, 39–48. [CrossRef]

14. Biswal, B.K.; Balasubramanian, R. Use of biochar as a low-cost adsorbent for removal of heavy metals from water and wastewater: A review. *J. Environ. Chem. Eng.* **2023**, *11*, 110986. [CrossRef]
15. Sultana, S.; Khairulet, I.; Hasan, M.A.; Khan, H.M.J.; Khan, M.A.R.; Deb, A.; Al Raihan, M.; Rahman, M.W. Adsorption of crystal violet dye by coconut husk powder: Isotherm, kinetics and thermodynamics perspectives. *Environ. Nanotechnol. Monit. Manag.* **2022**, *17*, 100651. [CrossRef]
16. Fouad, M.R. Physical characteristics and the Freundlich model of adsorption and desorption isotherm for fipronil in six types of Egyptian soil. *Curr. Chem. Lett.* **2023**, *12*, 207–216. [CrossRef]
17. Tejada-Tovar, C.; Villabona-Ortíz, A.; González-Delgado, Á. Adsorption Study of Continuous Heavy Metal Ions (Pb^{2+}, Cd^{2+}, Ni^{2+}) Removal Using Cocoa (*Theobroma cacao* L.) Pod Husks. *Materials* **2022**, *15*, 6937. [CrossRef]
18. Badawy, A.M.; Farghali, A.A.; Bonilla-Petriciolet, A.; Selim, A.Q.; Seliem, M.K. Effective removal of Cr(VI) and methyl orange by nano magnetite loaded starch/muscovite biocomposite: Characterization, experiments, advanced modeling, and physicochemical parameters interpretation. *Int. J. Biol. Macromol.* **2023**, *224*, 1052–1064. [CrossRef]
19. Agarwal, A.; Upadhyay, U.; Sreedhar, I.; Anitha, K.L. Simulation Studies of Cu(II) Removal from Aqueous Solution Using Olive Stone. *Clean. Mater.* **2022**, *5*, 100128. [CrossRef]
20. Nikam, S.; Mandal, D.; Dabhade, P. LDF Based Parametric Optimization to Model Fluidized Bed Adsorption of Trichloroethylene on Activated Carbon Particles. *Particuology* **2022**, *65*, 72–92. [CrossRef]
21. Shen, Y.; Shi, W.; Zhang, D.; Na, P.; Fu, B. The Removal and Capture of CO_2 from Biogas by Vacuum Pressure Swing Process Using Silica Gel. *J. CO2 Util.* **2018**, *27*, 259–271. [CrossRef]
22. Ezzati, R. Derivation of Pseudo-First-Order, Pseudo-Second-Order and Modified Pseudo-First-Order Rate Equations from Langmuir and Freundlich Isotherms for Adsorption. *Chem. Eng. J.* **2020**, *392*, 123705. [CrossRef]
23. Lavado-Meza, C.; De la Cruz-Cerrón, L.; Lavado-Puente, C.; Gamarra-Gómez, F.; Sacari-Sacari, E.; Dávalos-Prado, J.Z. Effective Removal of Cd(II) from Aqueous Solutions Using *Theobroma cacao* Agro-Industrial Waste. *Molecules* **2023**, *28*, 5491. [CrossRef]
24. Murthy, S.; Bali, G.; Sarangi, S.K. Effect of Lead on Metallothionein Concentration in Lead-Resistant Bacteria Bacillus Cereus Isolated from Industrial Effluent. *Afr. J. Biotechnol.* **2011**, *10*, 15966–15972. [CrossRef]
25. Murthy, S.; Bali, G. Lead biosorption by a bacterium isolated from industrial effluents. *Int. J. Microbiol. Res.* **2012**, *4*, 196–200. [CrossRef]
26. Upadhyay, U.; Gupta, S.; Agarwal, A.; Sreedhar, I.; Anitha, K.L. Adsorptive removal of Cd^{2+} ions using dolochar at an industrial-scale process optimization by response surface methodology. *Environ. Sci. Pollut. Res.* **2023**, *30*, 8403–8415. [CrossRef] [PubMed]
27. González-Delgado, Á.D.; Tejada-Tovar, C.; Villabona-Ortíz, A. Computer-aided Modeling and Evaluation of a Packed Bed for Chromium (vi) Removal using Residual Biomass of *Theobroma cacao* L. *Chem. Eng. Trans.* **2022**, *92*, 517–522. [CrossRef]
28. Ahmad, T.; Manzar, M.S.; Khan, S.; Al-Sharafi, M.A.; Georgin, J.; Franco, D.S.P.; Ullah, N. Enhanced adsorption of bisphenol-A from water through the application of isocyanurate based hyper crosslinked resin. *J. Mol. Liq.* **2024**, *395*, 123861. [CrossRef]
29. Benyahia, F.; O'Neill, K.E. Enhanced voidage correlations for packed beds of various particle shapes and sizes. *Part. Sci. Technol.* **2005**, *23*, 169–177. [CrossRef]
30. Lara, J.; Tejada, C.; Villabona, A.; Arrieta, A. Adsorción de Plomo y Cadmio En Sistema Continuo de Lecho Fijo Sobre Residuos de Cacao. *Rev. ION* **2017**, *29*, 111–122. [CrossRef]
31. Koua, B.K.; Koffi, P.M.E.; Gbaha, P. Evolution of Shrinkage, Real Density, Porosity, Heat and Mass Transfer Coefficients during Indirect Solar Drying of Cocoa Beans. *J. Saudi Soc. Agric. Sci.* **2019**, *18*, 72–82. [CrossRef]
32. Tejada-Tovar, C.; Lopez-Cantillo, K.; Vidales-Hernandez, K.; Villabona-Ortiz, A.; Acevedo-Correa, D. Kinetics and Bioadsortion Equilibrium of Lead and Cadmium in Batch Systems with Cocoa Shell (*Theobroma cacao* L.). *Contemp. Eng. Sci.* **2018**, *11*, 1111–1120. [CrossRef]
33. González-Delgado, Á.D.; Tejada-Tovar, C.; Villabona-Ortíz, A. Parametric Sensitivity Analysis of Chromium (Vi) Adsorption Using *Theobroma cacao* L Biomass via Process Simulation. *Chem. Eng. Trans.* **2022**, *92*, 535–540. [CrossRef]
34. Guan, Z.; Guo, Y.; Huang, Z.; Liao, X.; Chen, S.; Ou, X.; Sun, S.; Liang, J.; Cai, Y.; Xie, W.; et al. Simultaneous and Efficient Removal of Organic Ni and Cu Complexes from Electroless Plating Effluent Using Integrated Catalytic Ozonation and Chelating Precipitation Process in a Continuous Pilot-Scale System. *Chem. Eng. J.* **2022**, *428*, 131250. [CrossRef]
35. Zhang, N.; Xiao, J.; Bénard, P.; Chahine, R. Single- and Double-Bed Pressure Swing Adsorption Processes for H_2/CO Syngas Separation. *Int. J. Hydrogen Energy* **2019**, *44*, 26405–26418. [CrossRef]
36. Ali Abd, A.; Roslee Othman, M. Biogas Upgrading to Fuel Grade Methane Using Pressure Swing Adsorption: Parametric Sensitivity Analysis on an Industrial Scale. *Fuel* **2022**, *308*, 121986. [CrossRef]
37. Hameed, A.; Hameed, B.H.; Almomani, F.A.; Usman, M.; Ba-Abbad, M.M.; Khraisheh, M. Dynamic Simulation of Lead(II) Metal Adsorption from Water on Activated Carbons in a Packed-Bed Column. *Biomass Convers. Biorefinery* **2024**, *14*, 8283–8292. [CrossRef]

38. Ronda, A.; Martín-Lara, M.A.; Osegueda, O.; Castillo, V.; Blázquez, G. Scale-up of a packed bed column for wastewater treatment. *Water Sci. Technol.* **2018**, *77*, 1386–1396. [CrossRef]
39. Yasir, H.A.; Zein, S.H.; Holliday, M.C.; Jabbar, K.J.; Ahmed, U.; Jalil, A.A. Comparison of activated carbon and low-cost adsorbents for removal of 2,4-dichlorophenol from wastewater using Aspen Adsorption and response surface methodology. *Environ. Technol.* **2024**, *45*, 3029–3047. [CrossRef]

Disclaimer/Publisher's Note: The statements, opinions and data contained in all publications are solely those of the individual author(s) and contributor(s) and not of MDPI and/or the editor(s). MDPI and/or the editor(s) disclaim responsibility for any injury to people or property resulting from any ideas, methods, instructions or products referred to in the content.